◆ Human Brain Mapping 35:5701–5716 (2014) ◆

Encoding of Nested Levels of Acoustic Regularity in Hierarchically Organized Areas of the Human Auditory Cortex

Marc Recasens,[1,2] Sabine Grimm,[1,2] Andreas Wollbrink,[3] Christo Pantev,[3] and Carles Escera[1,2]*

[1]*Institute for Brain, Cognition and Behavior (IR3C), University of Barcelona, 08035 Catalonia, Spain*
[2]*Cognitive Neuroscience Research Group, Department of Psychiatry and Clinical Psychobiology, University of Barcelona, 08035 Catalonia, Spain*
[3]*Institute for Biomagnetism and Biosignalanalysis, University of Münster, 48149 Münster, Germany*

Abstract: Our auditory system is able to encode acoustic regularity of growing levels of complexity to model and predict incoming events. Recent evidence suggests that early indices of deviance detection in the time range of the middle-latency responses (MLR) precede the mismatch negativity (MMN), a well-established error response associated with deviance detection. While studies suggest that only the MMN, but not early deviance-related MLR, underlie complex regularity levels, it is not clear whether these two mechanisms interplay during scene analysis by encoding nested levels of acoustic regularity, and whether neuronal sources underlying local and global deviations are hierarchically organized. We registered magnetoencephalographic evoked fields to rapidly presented four-tone local sequences containing a frequency change. Temporally integrated local events, in turn, defined global regularities, which were infrequently violated by a tone repetition. A global magnetic mismatch negativity (MMNm) was obtained at 140–220 ms when breaking the global regularity, but no deviance-related effects were shown in early latencies. Conversely, Nbm (45–55 ms) and Pbm (60–75 ms) deflections of the MLR, and an earlier MMNm response at 120–160 ms, responded to local violations. Distinct neuronal generators in the auditory cortex underlay the processing of local and global regularity violations, suggesting that nested levels of complexity of auditory object representations are represented in separated cortical areas. Our results suggest that the different processing stages and anatomical areas involved in the encoding of auditory representations, and the subsequent detection of its violations, are hierarchically organized in the human auditory cortex. *Hum Brain Mapp 35:5701–5716, 2014.* © **2014 Wiley Periodicals, Inc.**

Key words: mismatch negativity; middle-latency responses; deviance detection; auditory cortex; magnetoencephalographic; beamforming

Contract grant sponsor: Spanish Ministry of Economy and Knowledge; Contract grant number: PSI2012-37174; Contract grant sponsor: Catalan Government; Contract grant number: SGR2009-11; Contract grant sponsor: ICREA Academia Distinguished Professorship (to C. E.)

*Correspondence to: Carles Escera, Cognitive Neuroscience Research Group, Department of Psychiatry and Clinical Psychobiology, University of Barcelona, P. Vall d'Hebron 171, 08035-Barcelona, Catalonia-Spain. E-mail: cescera@ub.edu

Received for publication 4 December 2013; Revised 29 April 2014; Accepted 28 June 2014.

DOI: 10.1002/hbm.22582

Published online 4 July 2014 in Wiley Online Library (wileyonlinelibrary.com).

INTRODUCTION

Sounds do not occur in isolation but are generally integrated into more complex patterns, as occurs in speech, animal vocalizations, or even in common sounds like our alarm ringtone. In such cases, the temporal integration of the ongoing sensory input plays an important role of organizing the acoustic background and, thus, guiding our perception [Bregman, 1990; Winkler et al., 2009]. Modeling our auditory scene in search for regularities is essential not only to organize our perceptual background into meaningful percepts but also to predict future sensory events [Friston, 2005; Winkler et al., 2009]. Hence, regularity-violation signals like the mismatch negativity (MMN), an auditory evoked potential to unexpected stimuli [Näätänen et al., 1978], serve as an appropriate tool to investigate the mechanism underlying perceptual organization and predictive processing in the human brain [Bendixen et al., 2012]. The MMN, generated in supratemporal areas between 100 and 250 ms after stimulus onset [Näätänen et al., 2007], indexes sudden changes in previously encoded regularities and is an indirect marker of the auditory memory-trace formation [Haenschel et al., 2005].

Remarkably, recent human studies have revealed the existence of earlier indices of deviance detection and regularity encoding preceding the MMN. Slabu et al. [2010] and Grimm et al. [2011] showed that different deflections of the middle-latency response (MLR), peaking between 10 and 50 ms after stimulus onset, were significantly enhanced in response to simple deviations as compared to control stimuli, suggesting that dynamic modeling of the acoustic regularity rather than adaptation underlies deviance detection well before MMN. In parallel, a large group of animal findings support the existence of very early indices of deviance detection in the mammal brain [Ayala et al., 2013; Taaseh et al., 2011]. Single-unit and multiunit recordings, as well as local field potentials, showed that particular auditory neurons display stimulus-specific adaptation (SSA), an attenuated response to repetitive stimuli, just 20 ms after sound onset [Malmierca et al., 2009; Ulanovsky et al., 2003]. Although SSA has been considered a possible single-neuron correlate of the MMN [Nelken and Ulanovsky, 2007], differences in the underlying pharmacological properties [Farley et al., 2010], the different anatomical generators involved [Malmierca et al. 2009], and their time scale, make MLR a better correlate of the animal SSA. Yaron et al. [2012] showed that neurons in the primary auditory cortex of the cat displayed a reduced firing when stimuli were presented in regular sequences, in contrast to typically random oddball sequences. Results showed that neural responses were sensitive to the structure of sound sequences; however, the decrease in neural discharge was present both in repeated and deviated stimuli, leaving open the question of whether early levels of the auditory pathway can encode complex or pattern-like regularities, and detect subsequent deviations. In humans, Cornella et al. [2012] showed that simple sound features like location are rapidly encoded at the level of MLR, and subsequently in the time range of the long-latency responses (LLR) by the MMN [Grimm et al., 2012; Sonnadara et al., 2006]. Notably, rare frequency repetitions in a sound alternation sequence were only detected at the level of MMN but not in earlier latencies. Similarly, results by Althen et al. [2013] showed that simple sound regularities (i.e., frequency) were processed earlier than complex regularities (i.e., frequency-location combinations). Together, the above mentioned findings suggest that regularity encoding is a ubiquitous property of the mammal auditory system that may be organized in ascending levels of complexity [Escera and Malmierca, 2014; Grimm and Escera, 2012]. However, two important points are still unresolved: First, previous human studies did not allow for testing whether deviance-related MLR and MMN mechanisms interplay when processing nested levels of regularity of growing complexity [Althen et al., 2013; Cornella et al., 2012], as occur in most real-life acoustic events. Second, it is not clear whether these mechanisms are supported by anatomically distinct areas and whether these sources show a hierarchical arrangement.

Previous studies have shown distinct MMN generators for simple rules as compared to more complex types of regularity. Magnetic mismatch negativity (MMNm) sources to deviations in feature conjunctions (i.e., pitch-location) have been located in more anterior portions of the auditory cortex when compared to sources derived from simple frequency changes [Takegata et al., 2000]. Similar results were obtained for abstract, but still local, changes in frequency direction [Korzyukov et al., 2003]. Alho et al. [1996] showed that equivalent current dipoles in response to changes in a serial tone pattern were located 1 cm medially as compared to sources of the MMNm elicited by simple frequency changes. Although accurate localization of the MMNm to complex changes might differ across studies depending on the stimuli used, the complexity of the regularity at play, or the source localization techniques used, overall findings suggest that the neural circuits underlying deviance detection vary as a function of the perceptual context [Alain et al. 1999a]. On this line, Sussman et al. [1998] showed that the MMN was abolished for predictable occurrences of a frequency change when tones in a sequence were presented at a fast pace. Their results suggest that sound organization changed from a local single-repeating tone rule to a global tone-repeating pattern. Despite that previous studies have elucidated the neuronal sources of both deviance-related MLR and MMNm [Recasens et al., 2014], as well as the generators underlying local and global deviations [Bekinschtein et al., 2009; Wacongne et al., 2011], this is, to our knowledge, the first attempt to localize multiple neuronal generators underlying local and global deviations in very early latencies during an unattended condition task.

In this magnetoencephalographic (MEG) study, we used similar sound structures to Yaron et al. [2012] and Sussman et al. [1998] with the difference that pattern

deviations (an unexpected tone repetition) were included in addition to local-rule deviations (a frequency change) [see also: Bekinschtein et al., 2009; Herholz et al., 2009, 2011; Wacongne et al., 2011]; therefore, putting the stress on both local (based on relations between temporary adjacent stimuli) and global (based on the relation between temporary nonadjacent sounds) types of regularity. We aimed to highlight the different roles of the early and late mechanisms in the organization of the auditory scene by showing that the neuronal generators underlying the representation of local and global invariance are mapped in distinct areas of the human brain and in distinct time scales, thus providing support for the notion that the human auditory system is organized in a hierarchical fashion. We expected to obtain an MMNm response to global regularity violations, thus indexing pattern-object representation, and early areas underlying MLR to respond to violations of local rules only; thus showing that beyond the acoustic feature at play, different auditory mechanisms assist the representation of local and global acoustic regularities. At the anatomical level, we hypothesized that multiple sources in the vicinity of the primary auditory cortex allocated the neuronal generators of local deviance detection as obtained in different time ranges [Recasens et al., 2014]. Moreover, we predicted that a clear anatomical separation would exist between sources underlying local and global acoustic regularity processing. We expected neuronal generators underlying global deviations to be located in hierarchically superior areas than those underlying local regularity violations.

MATERIALS AND METHODS

Participants

Fifteen healthy subjects (eight female, age: 27.4 ± 3, mean $\pm$ SD) participated in the experiment. All subjects had normal hearing as evaluated by clinical audiometry at the beginning of each MEG session for each ear. All subjects provided written consent prior to their participation in the study and received monetary compensation for it. The experimental protocol was approved by the ethics committee of the Medical Faculty of the University of Münster and the study was conducted according to the Declaration of Helsinki.

Stimuli and Procedure

Stimuli consisted of 50-ms pure tones (10 ms rise and decay time) delivered binaurally at 60 dB SL (Sensation level) via 90 cm long MEG-compatible plastic tubes (Etymotic Research). Two close sinusoidal tones, 988 Hz ("A" tone) or 880 Hz ("B" tone), were presented isochronously at 200 ms SOA (stimulus-onset-asynchrony) within repeating patterns of either four tones randomly occurring at a probability of 0.8 (AAA**B**: Standard patterns) or five tones occurring at a probability of 0.2 (AAA**a**B: Deviant patterns). The interval between global sequences was also kept at 200 ms, thus, leading to a continuously ongoing tone presentation. A fast presentation rate was used to facilitate automatic grouping of nested local objects under global patterns [Sussman et al., 1998; Sussman and Gumenyuk, 2005]. Additionally, a reversed block consisting of frequency-reversed standard patterns (BBB**A**) was presented to contrast against physically identical tones (Fig. 1). This prevented frequency-specific effects to mask real change-dependent effects, particularly for MLR. The global condition was assessed by comparing the activity from the rare fourth **a**-tone against the previous A-tone. We assessed the local condition by comparing the activity from local deviants, within standard patterns only, against physically identical standard tones preceding the frequency change. Thus, two local conditions, one per each frequency, were obtained (A vs. reversed-A; and B vs. reversed-B). In total, 660 rare repetitions of the **a**-tone (global deviants), 1992 B-tones (local deviants) in the oddball block, and 1105 A-tones in the reversed block (reversed local deviants) were delivered. Local deviants appearing after a global deviant were excluded from the analysis. The presentation of the experimental sequence was split in four pseudorandomized runs (consisting of three oddball blocks and one reversed block). Stimuli were presented using Presentation (Neurobehavioral Systems).

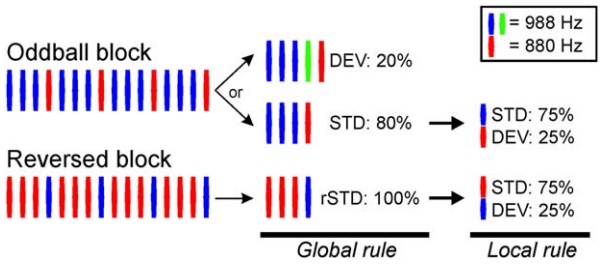

Figure 1.
Experimental design. Oddball and reversed blocks were composed of four-tone repeating sequences (200 ms SOA). Frequencies, and the role of deviant and standard, were interchanged in reversed blocks (left). Global rules (middle) were composed by sequences containing three repetitions and one pure tone deviation when standard (STD), and four repetitions and one pure tone deviation when deviants (DEV). The global deviation was defined by the fourth 988 Hz pure tone. Sequences in the reversed block contained standard global rules only (rSTD). Local rules (right) were defined by the pure tones within global sequences (standards only). Three standard repetitions (STD) defined the local rule, violated by a frequency change (DEV).

Data Acquisition and Analysis

Evoked magnetic fields were recorded with a 275-sensor whole-head system (OMEGA 2005, CTF Systems) in a magnetically shielded room. Data were acquired continuously

during each run with a sampling rate of 1200 Hz. Subjects were seated upright and were asked to relax, ignore acoustic stimulation and focus on a muted self-selected movie with no subtitles. The subject's alertness and compliance were verified by video monitoring. Recording lasted for 1 h approximately and subjects were not allowed to move their head between runs. No subjects were discarded due to head movement across runs (maximum head displacement throughout the session did not exceed 0.7 cm along the inferior–superior axis).

Analyses were carried out using the FieldTrip toolbox [Oostenveld et al., 2011] under Matlab 2012 (The MathWorks Inc.). For LLR analysis, datasets were epoched in intervals of 400 ms (100 ms baseline). Epoch intervals of 150 ms (50 ms baseline) were cut for MLR analysis. An offline band-pass filter (2-pass Butterworth, filter order of 4) was applied from 1 to 30 Hz for LLR, and from 15 to 150 Hz for MLR. Additionally, a DFT filter with 600 ms of sample padding was used to clean the data from the 50 Hz component and its harmonics. Epochs were baseline corrected using the whole baseline interval. On a separate analysis, the strongest components corresponding to cardiac and ocular artifacts were identified and rejected from the above mentioned dataset by means of independent component analysis, using the runica algorithm [Makeig et al., 1997]. To carry out independent component analysis, 100 samples (1 s length) from each run were downsampled and filtered between 1 and 150 Hz. A mean of 3.3 independent components per subject were rejected manually by visual inspection on the basis of their scalp topography and continuous activity [Jung et al., 2000]. Subsequent epochs containing channels having a signal amplitude range larger than 2.5 pT were considered artifact-contaminated and excluded from the averaging. To correct for intraindividual head position in the MEG sensor array across runs, artifact-free data were interpolated to a common sensor array template using a minimum-norm projection method [Knösche, 2002], and subsequently concatenated across runs. Remaining artifact-free epochs were averaged separately for each condition (global, local, and local-reversed). All subsequent analyses were performed separately for LLR and MLR.

Differences between deviant and standard events in each condition and latency were assessed nonparametrically using cluster-based permutation *t*-tests [for more details on the method see: Maris and Oostenveld, 2007]. This test controls for type I error rate in situations involving multiple comparisons (in our case, due to many comparisons of time-point by sensor). Moreover, this method requires no a priori hypotheses about the time intervals and distribution of the expected differences. Thus, we used this test in the sensor-space to determine, in an unbiased way, the presence of effects and the time windows where brain responses statistically differed between stimuli in each condition. Time windows showing significant effects were, then, used to reconstruct the activity in the source-space.

A planar gradient transformation of the axial gradiometer-recorded data were calculated by taking, for each sensor, the average of the absolute values of the first spatial derivatives in two orthogonal directions [Bastiaansen and Knösche, 2000]. Planar transformation simplified the interpretation of sensor-level results as it places a single field extrema right above the source [Hämäläinen et al., 1993]. Nonparametric statistical testing was applied on the transformed data to statistically compare deviant and standard stimuli in all possible conditions and latencies. Cluster-based permutation *t*-tests considered two dimensions, thus we assessed the existence of significant clusters of differential activity along the temporal (time-bin clusters) and spatial dimension (sensor clusters). For LLR, deviant and standard amplitude differences were assessed between 40 and 300 ms in steps of 20 ms. For MLR, a time window between 20 and 100 ms with steps of 5 ms was evaluated. A minimum of three neighboring significant sensors was required to form a significant cluster. Distance at which channels were considered neighbors was set in such a way that each channel had an average of 7.4 neighbors. Deviant and standard stimuli from the local and the local-reversed conditions were collapsed together prior to statistical analysis. A total amount of 1000 random permutations of the observed data were drawn and the critical alpha level for dependent-samples *t*-test (two-tailed, corrected) comparisons was set to 0.05. Only those conditions showing statistically significant differences in the sensor-space between deviant and standard stimuli in each time range were subsequently analyzed in source-space.

To obtain a more detailed localization, sources of evoked brain activity for standards and deviants were modeled using a time-domain spatial filter, the linearly constrained minimum variance (LCMV) beamformer [Van Veen et al., 1997]. Based on the segmentation of the brain surface of each individual's MRI, we obtained a semirealistic single-shell head model for each participant. Each brain volume had 5 mm resolution (23869 voxels inside the head). The leadfield matrix was computed for each grid voxel on the basis of a quasistatic approximation of the brain surface as a single shell [Nolte, 2003]. The weakest orthogonal component at each voxel of the leadfield matrix was excluded. To model the sources underlying each condition, we first computed common filter weights for LLR and MLR based on a balanced combination of deviant and standard responses in each condition (nontransformed data), thus ensuring that differences in source activity were not related to spatial filter differences. Therefore, the covariance matrix was computed on the average of 3000 trials derived from that combination. Power regularization was set to 1% of the mean power to maximize the sensitivity of the beamformer to focal sources. Subsequently, we projected nontransformed sensor-level data in each condition through the common spatial weights. The LCMV beamformer was independently

applied only on those statistically significant time intervals derived from the sensor-space analysis: the local MMNm (120–160 ms), global MMNm (160–200 ms), local Nbm (45–55), and local Pbm (60–75). Resulting source-space deviant and standard trials were averaged separately. Finally, source strengths were normalized using the neural activity index (NAI), where the estimated power at each grid point is divided by an estimate of the noise. Individual Pseudo-Z or NAI values were overlaid on the corresponding anatomical MRI. Anatomical and functional data were spatially normalized using SPM8 (Statistical Parametric Mapping; http://www.fil.ion.ucl.ac.uk/spm) to the MNI (Montreal Neurological Institute) template. Detailed determination of localization differences between the four deviance-related responses of interest (global MMNm, local MMNm, local Nbm, and local Pbm) was performed by means of analysis of variance (ANOVA) including the factor condition and hemisphere, independently for each of the three axes (*X*, *Y*, and *Z*). Individual single voxels showing the largest pseudo-Z values were retrieved from the beamformer source reconstructions thresholded at half-maximum. Additionally and as a measure of reliability, we repeated the same analysis using the 50 highest individual peak voxels (Top50) instead of the individual best voxel. Medial-lateral values were transformed into absolute values to assess hemispheric differences. For all statistical analyses, results were considered significant when $P < 0.05$. All post hoc comparisons were carried out using the Bonferroni correction for multiple comparisons. The Greenhouse–Geisser (G–G) correction was applied if the assumption of sphericity was violated. Effect sizes were reported for analyses of variance (partial eta squared, η_p^2) and post hoc comparisons (Cohen's *d*).

RESULTS

No statistical differences at any sensor were found between the local and the local-reversed difference waveforms (deviant minus standard: **A** vs. A = **B** vs. B), neither for LLR nor for MLR. Therefore, both conditions were merged and analyzed as a unique condition. In the LLR time range, local deviant and standard sounds at 120–140 ms elicited maximum activity on lateral and central scalp sensors (Fig. 2A, left and middle). Figure 2B, showing the time course of the root mean square (RMS) for deviant, standard, and their difference waveform, illustrates that local deviations elicited a statistically significant response between 120 and 160 ms after change onset ($P < 0.05$) when compared to local standards. Even though activity was higher on right hemisphere sensors, significant clusters of sensors emerged on both hemispheres (Fig. 2A, right). A smaller cluster of channels showing greater activity for deviant sounds as compared to standards emerged on right frontal areas between 240 and 260 ms. No clusters were found where standard stimuli elicited higher activity than deviant stimuli. In the LLR time range, infrequent repetitions of the standard tone, representing a global violation, elicited strong bilateral responses on lateral and central sensors between 160 and 180 ms (Fig. 3A, left and middle). Despite that maximum response activity for deviant and standard stimuli occurred between 160 and 180 ms, clusters of sensors showing significant ($P < 0.05$) global MMNm effects spanned from 140 to 220 ms after sound onset (Fig. 3B). Significant clusters were located bilaterally (Fig. 3A, right). No clusters were found where standard stimuli elicited higher activity than deviant stimuli. Additional clusters showing an enhanced activity ($P < 0.05$) for deviant stimuli were found between 240 and 280 ms, probably representing an enhanced response to local changes occurring after the rare global deviant within a deviant pattern. The same conditions were assessed throughout the MLR time range to identify whether early mechanisms of regularity encoding and change detection were functionally comparable to later mechanisms. Auditory tones elicited strong neuromagnetic activity over the scalp during the time intervals corresponding to the peaks of the typical MRL deflections: Nam (24.3 ms), Pam (32.6 ms), Nbm (46.4), and Pbm (62.5). For the local condition, statistically significant differences between deviant and standard tones emerged during the time course of the Nbm and Pbm waveforms, between 45 and 55 ms, and 60 and 75 ms after change onset, respectively (Fig. 4B). Both deviant and standard stimuli in the Nbm and Pbm time intervals showed maximum activity distributed bilaterally over lateral and central sensors (Fig. 4A, left and middle columns). For the Nbm component, clusters showing a significant differential activity ($P < 0.05$) appeared over left hemisphere sensors only (Fig. 4A, upper right). During the time interval of the Pbm component, significant clusters ($P < 0.05$) emerged on both hemispheres, (Fig. 4A, lower right). No clusters were found where standard stimuli elicited higher activity than deviant stimuli. Additional significant clusters ($P < 0.05$) emerged between 85 ms after change onset till the end of the epoch, probably reflecting an enhanced response to local deviants, as found in the LLR time range. For the global condition, auditory stimuli elicited strong evoked activity over the same time intervals as for local condition (Fig. 5A, left and middle columns); however, no significant differences were found between deviant and standard tones during the time course of MLR (Fig. 5A right column, and 5B).

Beamformer differential activity between local deviant and standard tones in the LLR time range (between 120 and 160 ms) yielded main sources of the local MMNm over anterior supratemporal cortices bilaterally (Fig. 6, first row). The peak voxel, showing the highest pseudo-Z value, on the right hemisphere was located on the anterior part of the superior temporal gyrus (STG, 64 −16 6), whereas a weaker peak activity on the left hemisphere overlapped areas of the middle temporal gyrus (MTG,

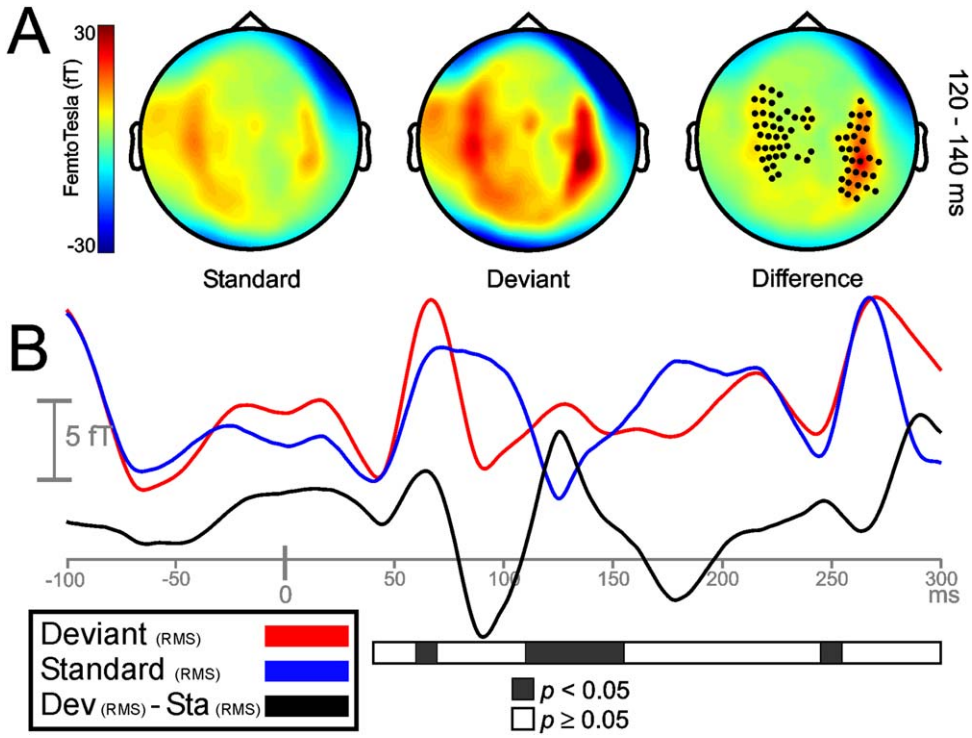

Figure 2.

Sensor-space activity for the local condition during LLR time range. **A**: The grand average of the topography of magnetic fields (planar transformed) between 120 and 140 ms after sound onset for standard (Sta), deviant (Dev), and their difference (Dev − Sta). Two bilateral clusters of sensors showed a significant increase in response to local frequency deviations ($P < 0.05$). **B**: Grand-averaged RMS waveforms (all sensors, not planar transformed) for deviant (red line), standard (blue line), and its difference RMS time course (black line). Black portions within the horizontal bar representing statistically significant time intervals ($P < 0.05$; in steps of 20 ms) show enhanced responses to deviant tones between 120 and 160 ms after the onset of the local deviation.

−60 −10 −6). Beamformer results for global deviants minus standard tones (between 160 and 200 ms) localized the generators of the global MMNm on posterior portions of the supratemporal cortex bilaterally (Fig. 6, second row). The peak voxel was located on posterior regions of the right STG (70 −34 16), and a weaker peak voxel on the left hemisphere fell on the posterior tip of STG (−64 −34 20). Using the same approach, we also investigated the location of neuronal sources underlying local regularity violations in the MLR time range. Sources of local deviants minus standard tones during the time interval of the Nbm MLR component (between 45 and 55 ms) were located bilaterally on supratemporal cortices. Consistent with sensor-level results (Fig. 4A), the left hemisphere showed stronger Pseudo-Z values than the right hemisphere (Fig. 6, third row). Peak voxels were located on the right anterior STG (66 −20 10) and the left post-central gyrus, just above the anterior tip of the left STG (−64 −20 14). During the time interval of the Pbm component (between 60 and 75 ms), beamformer results for the difference wave yielded bilateral activation on supratemporal regions, with the right hemisphere showing stronger pseudo-Z values (Fig. 6, fourth row). Peak voxels were located on the right (64 −10 4) and left (−66 −24 10) STG.

A more detailed analysis of the spatial differences between neuronal sources was carried out by examining the distribution, in each coordinate axis, of the individual peak voxels in each condition (Fig. 7). In these analyses, right hemisphere peak voxels from Subject 2 were excluded from all conditions on the basis that peak voxels in the *Y*-axis, for LLR conditions, were 1.5 standard deviations above the mean. The same type of analysis was repeated using the top 50 highest individual peak voxels in each condition to assess spatial differences in more detail. ANOVA of individual's highest peak voxels revealed a main effect of the condition in the *Y*-axis, indicating that individual peak voxels in the anterior–posterior axis differed between conditions ($F(3,39) = 16.29$, $P < 0.0001$, $\eta_p^2 = 0.56$). As no differences were found between hemispheres, data from the two hemispheres

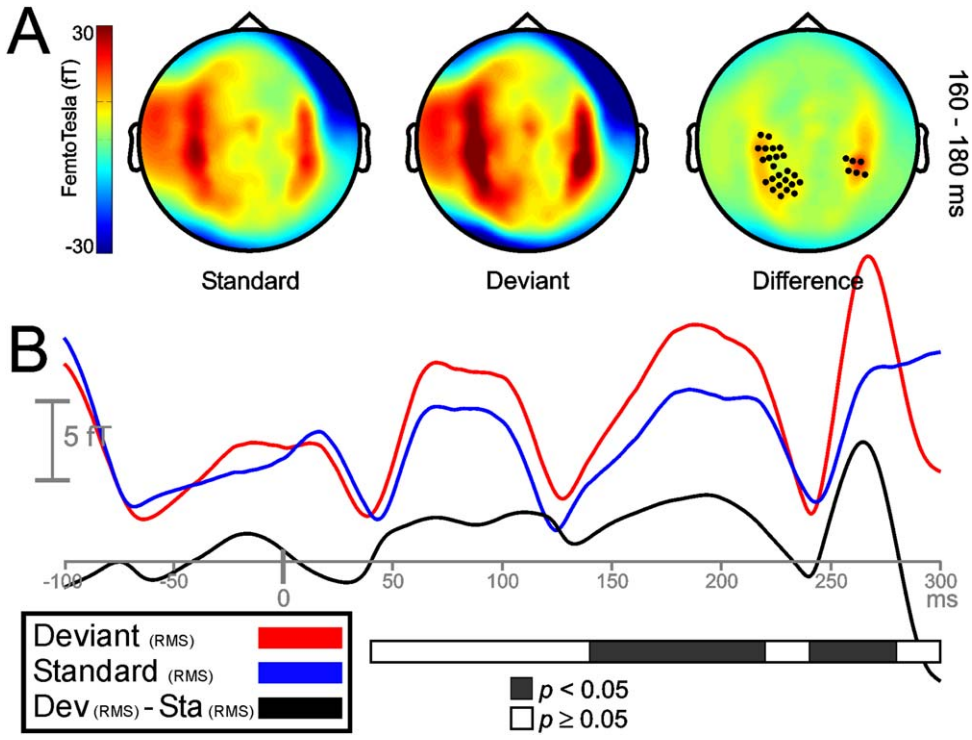

Figure 3.

Sensor-space activity for the global condition during LLR time range. **A**: The grand average of the topography of magnetic fields (planar transformed) between 160 and 180 ms after sound onset for standard (Sta), deviant (Dev), and their difference (Dev − Sta). Two bilateral clusters of sensors showed a significant increase in response to global frequency repetitions ($P < 0.05$). **B**: Grand-averaged RMS waveforms (all sensors, not planar transformed) for deviant (red line), standard (blue line), and its difference RMS time course (black line). Black portions within the horizontal bar representing statistically significant time intervals ($P < 0.05$; in steps of 20 ms) show enhanced responses to deviant tones between 140 and 220 ms after the onset of the global violation.

were collapsed for post hoc comparisons. Pairwise analyses showed that global MMNm peak voxels were located more posterior than the local MMNm ($t(28) = -6.01$, $P < 0.0001$, $d = 1.69$), Nbm ($t(28) = -3.37$, $P < 0.05$, $d = 0.77$), and Pbm ($t(28) = -4.75$, $P < 0.001$, $d = 1.28$). Local MMNm peak voxels were located significantly more anterior than those for the Nbm ($t(28) = 4.13$, $P < 0.005$, $d = 1.08$). The same procedure was repeated using the average coordinates from the best 50 individual peak voxels in each condition. This analysis showed an interaction between the factors condition and hemisphere ($F(3, 39) = 5.56$, $P < 0.01$, $\eta_p^2 = 0.3$). Separate analyses in each hemisphere showed that conditions differed significantly in the left hemisphere only ($F(3,42) = 28.12$, $P < 0.0001$ (G–G), $\eta_p^2 = 0.67$). Post hoc contrasts showed, for the left hemisphere, the same results reported using one single peak voxel, with the addition that local MMNm showed a more anterior location than Pbm ($t(14) = 5.35$, $P < 0.001$, $d = 1.98$). In the *Z*-axis, an interaction between the factors condition and hemisphere was found ($F(3,39) = 3.36$, $P < 0.05$, $\eta_p^2 = 0.21$). Separate analyses in each hemisphere showed that conditions differed significantly in the left ($F(3,42) = 11.96$, $P < 0.0001$, $\eta_p^2 = 0.46$) and right hemispheres ($F(3,39) = 5.15$, $P < 0.005$, $\eta_p^2 = 0.28$). Pairwise post hoc comparisons showed that the local MMNm was located significantly more inferior than global MMNm ($t(14) = 5.49$, $P < 0.0001$, $d = 1.37$), Nbm ($t(14) = 4.3$, $P < 0.005$, $d = 0.93$), and Pbm peak voxels in the left hemisphere ($t(14) = 3.99$, $P < 0.01$, $d = 0.89$). In the right hemisphere, only peak voxels in the global MMNm condition differed significantly from those in the Pbm condition ($t(13) = 3.48$, $P < 0.05$, $d = 0.89$). Identical results were found in the *Z*-axis when using the average of the Top50 individual peak voxels in each condition. Finally, no statistically significant differences were found in the *X*-axis when taking the best single peak voxel. However, Top50 analysis revealed a condition effect ($F(3, 39) = 4.73$, $P < 0.01$, $\eta_p^2 = 0.27$), and post hoc analysis, using collapsed

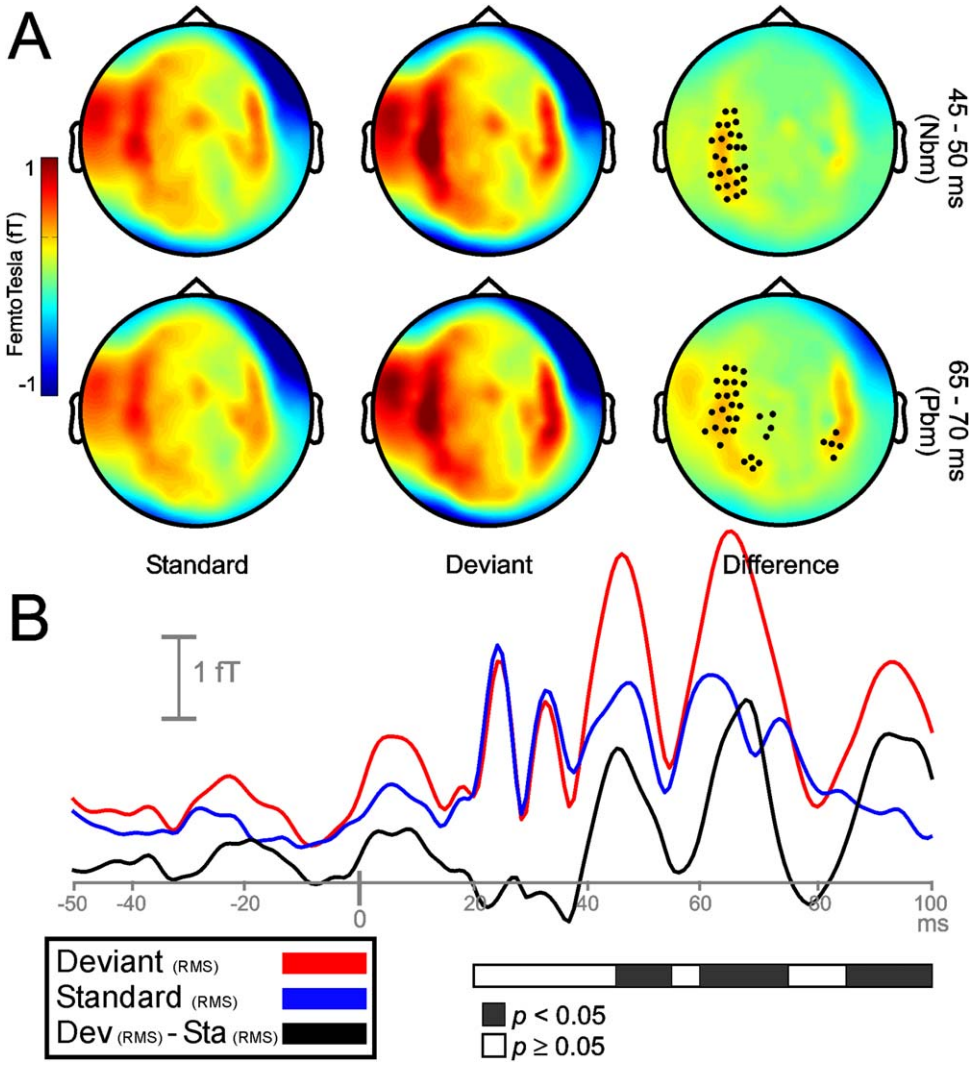

Figure 4.

Sensor-space activity for the local condition during MLR time range. **A**: The grand average of the topography of magnetic fields (planar transformed) between 45 and 50 ms (upper row), and between 65 and 70 ms (lower row) after sound onset for standard (Sta), deviant (Dev), and their difference (Dev − Sta). One cluster of sensors on left hemisphere for the Nbm component (upper row) and two bilateral clusters of sensors for the Pbm component (lower row) showed a significant increase in response to local frequency deviations ($P < 0.05$). **B**: Grand-averaged RMS waveforms (all sensors, not planar transformed) for deviant (red line), standard (blue line), and its difference RMS time course (black line). Black portions within the horizontal bar representing statistically significant time intervals ($P < 0.05$; in steps of 5 ms) show enhanced responses to deviant tones between 45 and 55 ms, and between 60 and 75 ms after the onset of the local violation.

data from the two hemispheres, showed statistically significant differences between Nbm and local MMNm peak voxels, the latter being more medial ($t(28) = 3.09$, $P < 0.05$, $d = 0.72$). In short, statistically significant local effects were found in the time intervals of the Nbm, Pbm, and MMNm, when comparing deviant and standard stimuli. No global effects were found in the time range of the MLR, and only a late MMNm response indexed global regularity violations. Source analysis of deviant minus standard tones for the aforementioned conditions revealed a significant spatial separation between neuronal sources underlying local and global regularity encoding mechanisms. Analyses revealed consistent differences in peak voxels' distribution along the inferior–superior and anterior–posterior axes. In addition, Top50 voxel analyses revealed that differences across conditions in the anterior–

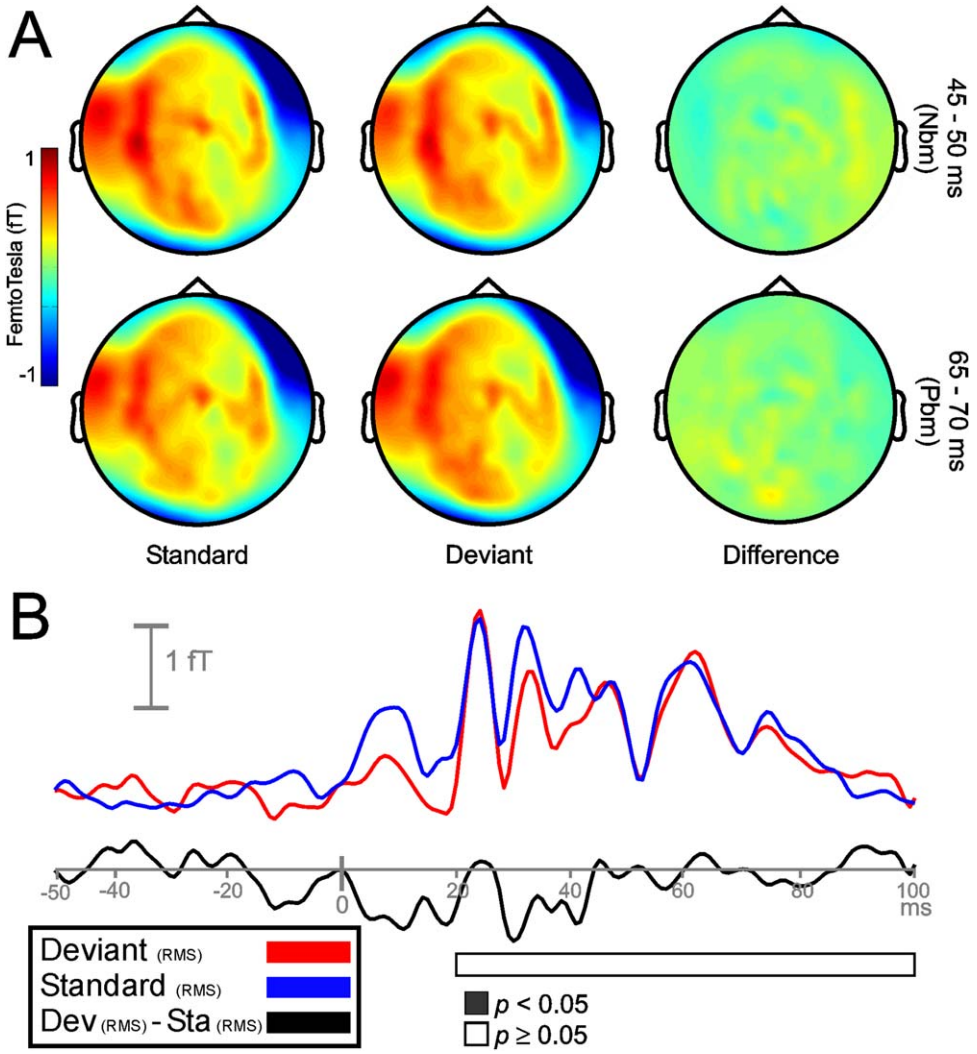

Figure 5.

Sensor-space activity for the global condition during MLR time range. **A**: The grand average of the topography of magnetic fields (planar transformed) between 45 and 50 ms (upper row), and between 65 and 70 ms (lower row) after sound onset for standard (Sta), deviant (Dev), and their difference (Dev − Sta). No cluster of sensors for any MLR deflections showed a significant increase in response to global frequency repetitions (n.s.). **B**: Grand-averaged RMS waveforms (all sensors, not planar transformed) for deviant (red line), standard (blue line), and its difference RMS time course (black line). Horizontal bar representing statistically significant time intervals (in steps of 5 ms) show the lack of significant differences between global deviant and standard tones.

posterior axis were carried by the left hemisphere mainly, and showed additional differences in the medial-lateral axis between MLR and LLR conditions.

DISCUSSION

Our results show that global regularity violations are indexed by a late MMNm (~160 ms) in the LLR time range, but not at earlier latencies during the time course of the MLRs. Likewise, we show that the processing of local rule violations is carried out in several time scales, in the LLR (~120 ms) and MLR (Nbm: ~45 ms, and Pbm: ~65 ms) time ranges. Source localization results describe a clear anatomical separation between neuronal sources allocating local and global types of regularity. Posterior areas in perisylvian region showed enhanced responses to global violations only, while anterior areas located near primary auditory cortices were only activated by local changes. Our results show that multiple anatomical regions in the

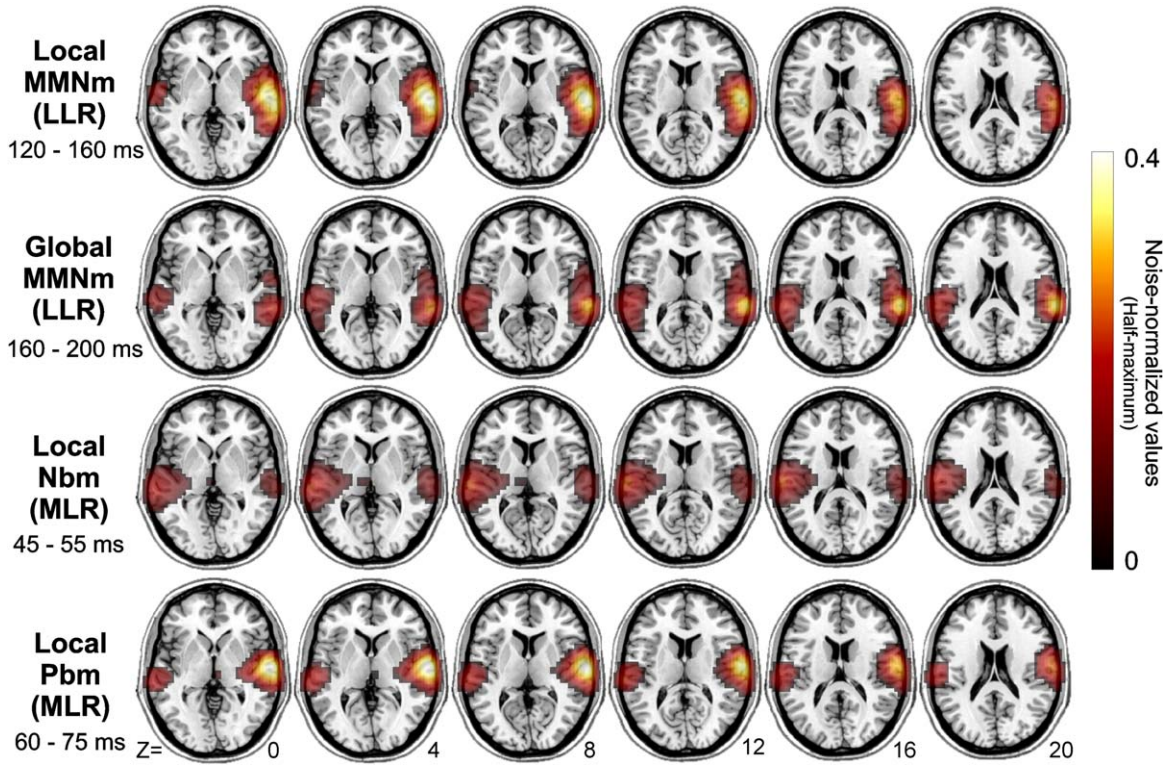

Figure 6.

Group-averaged source localization of the contrasts (deviant minus standard) for the four different conditions. The power (noise normalized pseudo-*Z* values) of the source representations is thresholded at half-maximum and overlaid onto the MNI standard brain. All conditions showed bilateral activation with main activity overlapping auditory regions. Only the global condition (second row), in the LLR time range, showed peak voxels localized in posterior regions of the supratemporal cortex. *Z* MNI coordinates (inferior–superior) are given at the lowest row on the corresponding slice.

auditory cortex sustain parallel sensitivities to different levels of acoustic regularity. We suggest that both early and late mechanisms of change detection are concurrently engaged during the processing of nested levels of sound organization, and their neural generators are located in separate auditory areas.

Enhanced responses to frequency changes occurred for MLR and LLR, indicating that the local regularity defined by the three repeated tones of each microsequence was extracted recursively in two consecutive and clearly separated time intervals. In accordance with these results, previous studies found MMNm responses to local violations in the LLR time range using a similar "global–local" experimental design [Bekinschtein et al., 2009; Herholz et al., 2009; Wacongne et al., 2011]. Sussman et al. [Sussman et al., 1998; Sussman and Gumenyuk, 2005] showed that a short SOA, as the one used here, abolished the MMN to local deviations when stimuli were presented in regular microsequences, suggesting that patterns were processed as a global entity. Disparate results between those studies and ours could be accounted for by the presence of interspersed global deviants acting as a contextual modification, and reactivating the dormant local regularity [Ritter et al., 1998; Sussman and Winkler, 2001]. The 200 ms SOA used in this study, lying right at the temporal edge for automatic grouping to occur [Sussman and Gumenyuk, 2005], might explain why a local MMNm still emerged in the reversed block where no global deviations were presented. In earlier time intervals, Nbm and Pbm waveforms of the MLR reflected deviance-related enhancements preceding MMNm. In consonance with our data, previous studies showed that spectral deviations elicit amplitude modulations in the Nbm component of the MLR [Alho et al., 2012; Althen et al., 2013; Grimm et al., 2011; Puschmann et al., 2013; Recasens et al., 2014]. Similarly, effects on the Pbm/P50m component have been previously interpreted as an indicator of gating-in, that is, a dishabituation to significant stimuli occurring after redundant stimulation [Boutros and Belger, 1999; Paraskevopoulos et al., 2012]. The early modulation of MLR in the local condition can be paralleled to animal findings showing very fast SSA to the repeated presentation of a particular frequency, and the subsequent increment in the response to deviant stimuli [Malmierca et al., 2009; Ulanovsky et al., 2003].

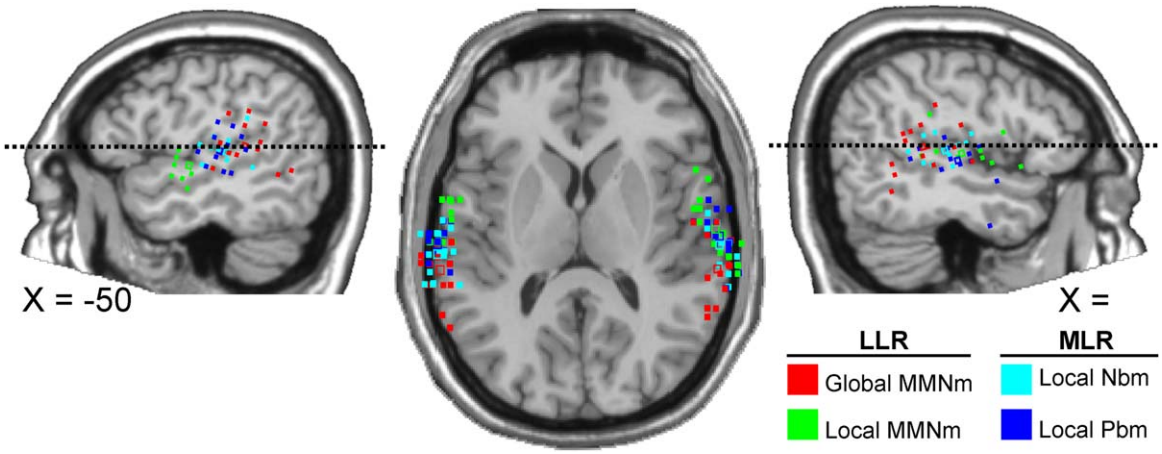

Figure 7.

Individual peak voxel locations for the four different conditions (deviant minus standard) superimposed on a template brain (Montreal Neurological Institute, MNI) tilted 16° down to assist the visualization of peak voxels on the supratemporal planes. Peak voxels are projected on one sagittal slice (lateral panels), thus omitting the *X*-axis; and on a tilted axial slice (central panel), thus omitting the *Z*-axis coordinate. Dotted lines on sagittal views indicate the height of the axial slice.

With regard to the global condition, our results are in line with previous research showing mismatch-like responses to infrequent sound repetitions [Alain et al., 1994, 1999b; Boh et al., 2011; Chait et al., 2008; Herholz et al., 2009, 2011; Horvath et al., 2001; Tervaniemi et al., 2001]. Previous attempts to probe complex regularity processing in the MLR and LLR range designed complex regularities based on feature combinations [Althen et al., 2013] or simple patterns, whose regularity was defined by the interrelationship of adjacent tones [Cornella et al., 2012]. Here, we tested complex regularity processing and early deviance detection using nested and more realistic acoustic events. The global MMNm indicates the presence of temporally integrated stimulus representations, which could correspond to the subjective pattern percept [Näätänen and Winkler, 1999]. Recent studies using similar global–local paradigms and active listening tasks have investigated the conscious processing of global regularities [Bekinschtein et al., 2009; Wacongne et al., 2011] discovering that a P3b, but not MMN, was elicited during global violations. Dissimilarities in the responses indexing global changes (global MMN or P3b) between Bekinschtein et al. [2009] and other studies including ours [see also: Herholz et al., 2009, 2011; Horvath et al., 2001] might be accounted for by the different task demands. In this line, our results support that active or conscious listening is not a prerequisite for the automatic encoding of global regularities and that different brain mechanisms might be involved in the automatic processing of global regularity violations. It is worth noting that a sustained field between about 50 and 130 ms, with a dipolar field equivalent to the P50/P1 EEG response, characterized the time course of the standards and repetition violations, but not that of the frequency deviants. Such differences in spatial distribution, which are probably explained by the fast and regular presentation rate, could reflect the distinct neuronal generators involved in the processing of local and global deviations [Lütkenhöner, 2003]. The absence of earlier activity preceding the global MMNm is in line with previous findings showing that sound transitions from a regular sequence to a constant pure-tone elicited a peak at 160 ms after transition but no earlier activity in the P50 time range, suggesting that early mechanisms of deviance detection may be limited by the kinds of regularity they can compute [Chait et al., 2008]. Based on the lack of global deviance-related effects in the time range of the MLR, we suggest that very early deviance detection mechanisms work, at least for frequency [Leung et al., 2012], at the feature level [Alho et al., 2012; Althen et al., 2011; Grimm et al., 2012; Leung et al., 2013], and reflect an early stage prior to feature combination, sequential grouping, or the extraction of regularities based on the interrelationship between sounds. In sum, our study refine previous findings by Cornella et al. [2012] and Althen et al. [2013] and provide additional evidence showing that deviance detection is hierarchically organized consistently with the level of complexity in which the auditory input can be organized. In other words, the detection of simple regularities is already accomplished at early stages of the auditory hierarchy, in the time range of the MLR, whereas complex levels of regularity are encoded in higher levels along the novelty system's hierarchy [Escera and Malmierca, 2014].

Source reconstruction revealed neuronal generators that were consistent with sensor-level data, pointing to the overall robustness of beamforming results. As expected, sources of MMNm and deviance-related MLR deflections to local deviations were located on anterior areas of STG and lateral aspects of HG (Heschl's gyrus) bilaterally

[Doeller et al., 2003; Inui et al., 2006; Opitz et al., 1999; Schönwiesner et al., 2007; Yvert et al., 2001]. Consistent with sensor-level data and previous findings, MMNm was larger on the right hemisphere [Paavilainen et al., 1991; Recasens et al., 2014]. Similarly, left- and right-ward lateralization of deviance-related effects in the Nbm and Pbm components, respectively, was in agreement with sensor-level data. The individual peak-voxel distribution for the different local conditions (deviance-related MLR and MMN) revealed a spatial separation along the sylvian fissures between very early deviance-related Nbm sources and MMNm sources to local changes. That difference was even clearer on the left hemisphere, where MMNm neuronal sources were located more inferior than deviance-related MLR sources. Our results replicate previous localization results obtained by Recasens et al. [2014] showing a mediolateral and anterior–posterior separation between MLR and MMNm sources. The lack of differences in the mediolateral axis might be accounted for by the different sensitivity of axial gradiometers to deep sources as compared to magnetometers [Hämäläinen et al., 1993]. Anterior MMNm sources, as compared to N1m generators, have been reported by classic MMN studies using small frequency separations. Jääskeläinen et al. [2004] showed that such source configuration could be explained by the relatively different adaptation sensitivity of anterior and posterior N1m sources. Using similar paradigms, focal activation in or near primary auditory cortex has been previously reported for local MMN [Bekinschtein et al., 2009; Wacongne et al., 2011]. Uhrig et al. [2014] registered fMRI in the monkey brain also revealing a much more distributed cortical network for local novelties that included subcortical nuclei and primary auditory cortices. In agreement, our findings suggest that multiple loci near HG support the processing of local events in successive time intervals. Sources underlying violations of the global regularity were located in posterior STG, or planum temporale (PT), more posterior than neuronal activity underlying all remaining local conditions. Our data agree with previous findings suggesting that physical dimensions-like frequency and more complex regularities are encoded in distinct auditory areas [Alain et al., 1999a; Alho et al., 1996; Levänen et al., 1996]. Previous studies revealed the involvement of a global workspace network during the processing of global rule violations that included auditory, prefrontal, parietal, and cingulate regions [Bekinschtein et al., 2009; Wacongne et al., 2011]. Even though strong parallelisms with our source reconstruction results should be avoided since P3b was elicited in these studies, Uhrig et al. [2014] showed the involvement of posterior auditory regions, the temporo-parietal area, in the preprocessing of global violations. This posterior localization for pattern processing, understood as sequences of sounds unfolding on a multidimensional space [Bregman, 1990], can be related to neuroimaging findings showing auditory and motor interactions during rhythm processing [Chen et al., 2009]. PT is frequently reported during auditory spatial tasks as part of the dual-stream model [Alain et al., 2001; Rauschecker and Tian, 2000], which has been criticized as over-simplistic [Belin and Zatorre, 2000; Hall, 2003], and recently re-examined as an auditory-action related area [for a review see: Arnott and Alain, 2011]. Thus, posterior STG activation might reflect the spectrotemporal analysis of complex sounds sequences [Zatorre et al., 2002] or the breaking of previously encoded auditory-motor representation of the global sequence [Chen et al., 2009; Karabanov et al., 2009]. Under the dual-stream framework, findings showing sources underlying intelligible speech processing located in anterior portions of the superior temporal sulcus [Evans et al., in press; Scott et al., 2000] could be explained in terms of a ventral pathway involved in mapping sound into meaning, and a dorsal pathway involved in mapping sound into an articulatory-based representation [Arnott and Alain, 2011; Hickok and Poeppel, 2007]. In line, Griffiths and Warren [2002] suggested that PT contains mechanisms for parsing the different types of auditory information included in complex sounds, which work in a template-matching fashion [Näätänen et al., 2005; Winkler et al., 2009]. In sum, source localization results are in agreement with a putative role of posterior STG in the encoding of discrete local units into an ordered and extended global auditory signal [Warren et al., 2005]. Our results suggest that while different anterior regions participate in the encoding of features at the local level, posterior and hierarchically superior regions may be engaged in the encoding of more complex or global patterns. Despite converging evidence shows the existence of MMN generators in the frontal lobe [Doeller et al., 2003; Schönwiesner et al., 2007], no frontal areas were observed in this study. Previous studies described the involvement of frontal regions when using listening tasks and by recording EEG or intracranial activity during global–local paradigms [Bekinschtein et al., 2009; Chennu et al., 2013]. However, MEG findings, or the lack of them, suggest that the frontal MMNm component is either located deeper in the brain or is radially oriented and, hence, almost silent to MEG sensors [Hämäläinen et al., 1993; Rinne et al., 2000]. More sophisticated source analyses (e.g., using regions of interest) or design parameters might allow future studies to reveal frontal generators using MEG.

A long debate exists about whether MMN can be explained solely on the differential states of refractoriness of neurons specifically responding to given stimulus attributes that characterize the standard sound [May and Tiitinen, 2010], or denotes a predictive coding mechanism supported by genuine memory-based comparisons between a deviant input and the previously encoded regularity [Jacobsen and Schröger, 2001; Näätänen et al., 2005; Winkler et al., 2009]. Although both alternatives are not mutually exclusive, several conditions controlling for stimulus probability have been designed to differentiate

adaptation from genuine memory-based effects in the MMN response [Jacobsen and Schröger, 2001; Jacobsen et al., 2003; Ruhnau et al., 2012; Schröger and Wolff, 1996]. Given that this study did not implement such a condition, it may be argued that one cannot be sure whether "sensory" or "cognitive" deviance detection mechanisms [Opitz et al., 2005] are participating in the local effects of both MLR and LLR. However, our previous research using controlled designs showed that genuine deviance detection is preserved in both LLR and MLR time ranges for rare changes in frequency or location [Grimm et al., 2011, 2012; Slabu et al., 2010, 2012]. Also Wacongne et al. [2011] showed that novelty responses to local violations remain present when the final sound is omitted, an effect that cannot be explained under the adaptation hypothesis. Nevertheless, an alternative interpretation of our local effects is that amplitude enhancements indexed stimulus change per se, irrespective of the previously encoded regularity, and hence, acted as a simple stimulus detector signaling to higher-order mechanisms [Recasens et al., 2014]. Similar interpretations have been offered by previous studies suggesting that early deflections index a sensory change detection mechanism based on differential states of refractoriness during a "minimal integration window," and later MMN responses reflect the construction of a new memory-trace based regularity [Chait et al., 2007, 2008]. Similarly, Schönwiesner et al. [2007] found that only high-order regions in the temporal cortex were sensitive to the magnitude of deviation whereas hierarchically lower areas were not, suggesting that medial portions of the HG are devoted to a nonmemory-based mechanism of change detection. Regarding the global effects, an interpretation based on the different refractory states for deviant and standard responses could not be applied. Whereas a higher degree of adaptation was expected for the global deviant, the rare four-tone repetition, an enhanced response was obtained indicating that global regularities were extracted and its deviations detected in spite of the expected greater degree of adaptation. In sum, local violations presented here are likely reflecting a combination of genuine memory-based and refractoriness effects, whereas global rules are probably extracted by means of more complex memory-based processes. Nevertheless, beyond the underlying neurophysiological mechanism that triggers deviance detection, the hierarchical notion we support is in agreement with the ideas of Schönwiesner et al. [2007] proposing different roles for hierarchically distinct areas involved in the MMN generation process, namely the detection of changes in global as opposed to local regularities. Our suggestion that early and late regularity encoding and deviance detection mechanisms work in a parallel fashion is based on the fact that hierarchically inferior regions of the auditory cortex sustain local rules (frequency invariance), and respond to local deviations; Concurrently with the presentation of the same stimulus, higher-order regions do not show enhanced responses, as local deviations represent an integral part of the global regularity template. In line with Bregman's [1990] view of multiple preattentive processes that analyze the input in parallel, our source reconstruction results support the notion that a late MMNm to global changes, located in posterior areas of the auditory cortex, underlies an unconscious mechanism that organizes regularity inputs into meaningful objects, while representation of necessary local features is concurrently maintained in hierarchically lower levels.

CONCLUSIONS

This study proposes that temporally and spatially distinct deviance detection mechanisms underlie growing levels of regularity encoding in the human auditory system, which in turn, support parallel levels of acoustic organization. Using sequences composed of interrelated sounds, with local deviants nested into global patterns, we showed that only late mechanisms of deviance detection reflect the spectrotemporal integration of single events into a global organization. Noteworthy, anterior areas near primary auditory cortex, and posterior regions in PT, interplay to maintain local and global sensory representations, thus showing that different regularity levels are encoded in parallel within hierarchically organized regions of the human auditory cortex.

REFERENCES

Alain C, Woods D, Ogawa K (1994): Brain indices of automatic pattern processing. Neuroreport 6:140–144.

Alain C, Achim A, Woods DL (1999a): Separate memory-related processing for auditory frequency and patterns. Psychophysiology 36:737–744.

Alain C, Cortese F, Picton TW (1999b): Event-related brain activity associated with auditory pattern processing. Neuroreport 10: 2429–2434.

Alain C, Arnott SR, Hevenor S, Graham S, Grady CL (2001): "What" and "where" in the human auditory system. Proc Natl Acad Sci USA 98:12301–12306.

Alho K, Tervaniemi M, Huotilainen M, Lavikainen J, Tiitinen H, Ilmoniemi R, Knuutila J, Näätänen R (1996): Processing of complex sounds in the human auditory cortex as revealed by magnetic brain responses. Psychophysiology 33:369–375.

Alho K, Grimm S, Mateo-León S, Costa-Faidella J, Escera C (2012): Early processing of pitch in the human auditory system. Eur J Neurosci 36:2972–2978.

Althen H, Grimm S, Escera C (2011): Fast detection of unexpected sound intensity decrements as revealed by human evoked potentials. PLoS One 6:e28522.

Althen H, Grimm S, Escera C (2013): Simple and complex acoustic regularities are encoded at different levels of the auditory hierarchy. Eur J Neurosci 38:3448–3455.

Arnott SR, Alain C (2011): The auditory dorsal pathway: Orienting vision. Neurosci Biobehav Rev 35:2162–2173.

Ayala YA, Pérez-González D, Duque D, Nelken I, Malmierca MS (2013): Frequency discrimination and stimulus deviance in the inferior colliculus and cochlear nucleus. Front Neural Circuits 6:119.

Bastiaansen MC, Knösche TR (2000): Tangential derivative mapping of axial MEG applied to event-related desynchronization research. Clin Neurophysiol 111:1300–1305.

Bekinschtein T, Dehaene S, Rohaut B, Tadel F, Cohen L, Naccache L (2009): Neural signature of the conscious processing of auditory regularities. Proc Natl Acad Sci USA 106:1672–1677.

Belin P, Zatorre R (2000): "What", "where" and "how" in auditory cortex. Nat Neurosci 3:965–966.

Bendixen A, SanMiguel I, Schröger E (2012): Early electrophysiological indicators for predictive processing in audition: A review. Int J Psychophysiol 83:120–131.

Boh B, Herholz SC, Lappe C, Pantev C (2011): Processing of complex auditory patterns in musicians and nonmusicians. PLoS One 6:e21458.

Boutros NN, Belger A (1999): Midlatency evoked potentials attenuation and augmentation reflect different aspects of sensory gating. Biol Psychiatry 45:917–922.

Bregman AS (1990): Auditory Scene Analysis: The Perceptual Organization of Sound. Cambridge MA: MIT Press.

Chait M, Poeppel D, de Cheveigné A, Simon JZ (2007): Processing asymmetry of transitions between order and disorder in human auditory cortex. J Neurosci 27:5207–5214.

Chait M, Poeppel D, Simon JZ (2008): Auditory temporal edge detection in human auditory cortex. Brain Res 1213:78–90.

Chen JL, Penhune VB, Zatorre R (2009): The role of auditory and premotor cortex in sensorimotor transformations. Ann N Y Acad Sci 1169:15–34.

Chennu S, Noreika V, Gueorguiev D, Blenkmann A, Kochen S, Ibáñez A, Owen AM, Bekinschtein TA (2013): Expectation and attention in hierarchical auditory prediction. J Neurosci 33: 11194–11205.

Cornella M, Leung S, Grimm S, Escera C (2012): Detection of simple and pattern regularity violations occurs at different levels of the auditory hierarchy. PLoS One 7:e43604.

Doeller C, Opitz B, Mecklinger A, Krick C, Reith W, Schröger E (2003): Prefrontal cortex involvement in preattentive auditory deviance detection: Neuroimaging and electrophysiological evidence. Neuroimage 20:1270–1282.

Escera C, Malmierca MS (2014): The auditory novelty system: An attempt to integrate human and animal research. Psychophysiology 51:111–123.

Evans S, Kyong JS, Rosen S, Golestani N, Warren JE, McGettigan C, Mourão-Miranda J, Wise RJ, Scott SK: The pathways for intelligible speech: Multivariate and univariate perspectives (in press).

Farley BJ, Quirk MC, Doherty JJ, Christian EP (2010): Stimulus-specific adaptation in auditory cortex is an NMDA-independent process distinct from the sensory novelty encoded by the mismatch negativity. J Neurosci 30:16475–16484.

Friston K (2005): A theory of cortical responses. Philos Trans R Soc B Biol Sci 360:815–836.

Griffiths TD, Warren JD (2002): The planum temporale as a computational hub. Trends Neurosci 25:348–253.

Grimm S, Escera C (2012): Auditory deviance detection revisited: Evidence for a hierarchical novelty system. Int J Psychophysiol 85:88–92.

Grimm S, Escera C, Slabu L, Costa Faidella J (2011): Electrophysiological evidence for the hierarchical organization of auditory change detection in the human brain. Psychophysiology 48: 377–384.

Grimm S, Recasens M, Althen H, Escera C (2012): Ultrafast tracking of sound location changes as revealed by human auditory evoked potentials. Biol Psychol 89:232–239.

Haenschel C, Vernon DJ, Dwivedi P, Gruzelier JH, Baldeweg T (2005): Event-related brain potential correlates of human auditory sensory memory-trace formation. J Neurosci 25:10494–10501.

Hall D (2003): Auditory pathways: Are "What" and "Where" appropriate? Curr Biol 13:R406–R408.

Hämäläinen M, Hari R, Ilmoniemi RJ, Knuutila J, Lounasmaa O (1993): Magnetoencephalography—Theory, instrumentation, and applications to noninvasive studies of the working human brain. Rev Mod Phys 65:413–497.

Herholz SC, Lappe C, Pantev C (2009): Looking for a pattern: An MEG study on the abstract mismatch negativity in musicians and nonmusicians. BMC Neurosci 10:42.

Herholz SC, Boh B, Pantev C (2011): Musical training modulates encoding of higher-order regularities in the auditory cortex. Eur J Neurosci 34:524–529.

Hickok G, Poeppel D (2007): The cortical organization of speech processing. Nat Rev Neurosci 8:393–402.

Horvath J, Czigler I, Sussman E, Winkler I (2001): Simultaneously active pre-attentive representations of local and global rules for sound sequences in the human brain. Brain Res brain Res 12:131–144.

Inui K, Okamoto H, Miki K, Gunji A, Kakigi R (2006): Serial and parallel processing in the human auditory cortex: A magnetoencephalographic study. Cereb cortex 16:18–30.

Jääskeläinen IP, Ahveninen J, Bonmassar G, Dale AM, Ilmoniemi RJ, Levänen S, Lin FH, May P, Melcher J, Stufflebeam SM, Tiitinen H, Belliveau JW (2004): Human posterior auditory cortex gates novel sounds to consciousness. Proc Natl Acad Sci USA 101:6809–6814.

Jacobsen T, Schröger E (2001): Is there pre-attentive memory-based comparison of pitch? Psychophysiology 38:723–727.

Jacobsen T, Schröger E, Horenkamp T, Winkler I (2003): Mismatch negativity to pitch change: Varied stimulus proportions in controlling effects of neural refractoriness on human auditory event-related brain potentials. Neurosci Lett 344:79–82.

Jung TP, Makeig S, Westerfield M, Townsend J, Courchesne E, Sejnowski TJ (2000): Removal of eye activity artifacts from visual event-related potentials in normal and clinical subjects. Clin Neurophysiol 111:1745–1758.

Karabanov A, Blom O, Forsman L, Ullén F (2009): The dorsal auditory pathway is involved in performance of both visual and auditory rhythms. Neuroimage 44:480–488.

Knösche TR (2002): Transformation of whole-head MEG recordings between different sensor positions. Biomed Tech (Berl) 47: 59–62.

Korzyukov O, Winkler I, Gumenyuk V, Alho K (2003). Processing abstract auditory features in the human auditory cortex. Neuroimage 20:2245–2258.

Leung S, Cornella M, Grimm S, Escera C (2012): Is fast auditory change detection feature specific? An electrophysiological study in humans. Psychophysiology 49:933–942.

Leung S, Recasens M, Grimm S, Escera C (2013): Electrophysiological index of acoustic temporal regularity violation in the middle latency range. Clin Neurophysiol 124:2397–2405.

Levänen S, Ahonen A, Hari R, McEvoy L, Sams M (1996): Deviant auditory stimuli activate human left and right auditory cortex differently. Cereb Cortex 6:288–296.

Lütkenhöner B (2003): Magnetoencephalography and its Achilles' heel. J Physiol Paris 97:641–658.

Makeig S, Jung TP, Bell AJ, Ghahremani D, Sejnowski TJ (1997): Blind separation of auditory event-related brain responses into independent components. Proc Natl Acad Sci USA 94:10979–10984.

Malmierca MS, Cristaudo S, Pérez-González D, Covey E (2009): Stimulus-Specific adaptation in the inferior colliculus of the anesthetized rat. J Neurosci 29:5483–5493.

Maris E, Oostenveld R (2007): Nonparametric statistical testing of EEG- and MEG-data. J Neurosci Methods 164:177–190.

May PJ, Tiitinen H (2010): Mismatch negativity (MMN), the deviance-elicited auditory deflection, explained. Psychophysiology 47:66–122.

Näätänen R, Winkler I (1999): The concept of auditory stimulus representation in cognitive neuroscience. Psychol Bull 125:826–859.

Näätänen R, Gaillard AW, Mantysalo S (1978): Early selective-attention effect on evoked potential reinterpreted. Acta Psychol 42:313–329.

Näätänen R, Jacobsen T, Winkler I (2005): Memory-based or afferent processes in mismatch negativity (MMN): A review of the evidence. Psychophysiology 42:25–32.

Näätänen R, Paavilainen P, Rinne T, Alho K (2007): The mismatch negativity (MMN) in basic research of central auditory processing: A review. Clin Neurophysiol 118:2544–2590.

Nelken I, Ulanovsky N (2007): Mismatch negativity and stimulus-specific adaptation in animal models. J Psychophysiol 21:214–223.

Nolte G (2003): The magnetic lead field theorem in the quasi-static approximation and its use for magnetoencephalography forward calculation in realistic volume conductors. Phys Med Biol 48:3637–3652.

Oostenveld R, Fries P, Maris E, Schoffelen J-M (2011): FieldTrip: Open source software for advanced analysis of MEG, EEG, and invasive electrophysiological data. Comput Intell Neurosci 2011:156869.

Opitz B, Mecklinger A, von Cramon DY, Kruggel F (1999): Combining electrophysiological and hemodynamic measures of the auditory oddball. Psychophysiology 36:142–147.

Opitz B, Schröger E, von Cramon D (2005): Sensory and cognitive mechanisms for preattentive change detection in auditory cortex. Eur J Neurosci 21:531–535.

Paavilainen P, Alho K, Reinikainen K, Samsi M, Näätänen R (1991): Right-hemisphere dominance of different mismatch negativities. Electroencephalogr Clin Neurophysiol 78:466–479.

Paraskevopoulos E, Kuchenbuch A, Herholz SC, Pantev C (2012): Statistical learning effects in musicians and non-musicians: An MEG study. Neuropsychologia 50:341–349.

Puschmann S, Sandmann P, Ahrens J, Thorne J, Weerda R, Klump G, Debener S, Thiel CM (2013): Electrophysiological correlates of auditory change detection and change deafness in complex auditory scenes. Neuroimage 75:155–164.

Rauschecker JP, Tian B (2000): Mechanisms and streams for processing of "what" and "where" in auditory cortex. Proc Natl Acad Sci USA 97:11800–11806.

Recasens M, Grimm S, Capilla A, Nowak R, Escera C (2014): Two sequential processes of change detection in hierarchically ordered areas of the human auditory cortex. Cereb Cortex 24:143–153.

Rinne T, Alho K, Ilmoniemi RJ, Virtanen J, Näätänen R (2000): Separate time behaviors of the temporal and frontal mismatch negativity sources. Neuroimage 12:14–9.

Ritter W, Gomes H, Cowan N, Sussman E, Vaughan HG (1998): Reactivation of a dormant representation of an auditory stimulus feature. J Cogn Neurosci 10:605–614.

Ruhnau P, Herrmann B, Schröger E (2012): Finding the right control: The mismatch negativity under investigation. Clin Neurophysiol 123:507–512.

Schönwiesner M, Novitski N, Pakarinen S, Carlson S, Tervaniemi M, Näätänen R (2007): Heschl's gyrus, posterior superior temporal gyrus, and mid-ventrolateral prefrontal cortex have different roles in the detection of acoustic changes. J Neurophysiol 97:2075–2082.

Schröger E, Wolff C (1996): Mismatch response of the human brain to changes in sound location. Neuroreport 7:3005–3008.

Scott SK, Blank CC, Rosen S, Wise RJ (2000): Identification of a pathway for intelligible speech in the left temporal lobe. Brain 123:2400–2406.

Slabu L, Escera C, Grimm S, Costa-Faidella J (2010): Early change detection in humans as revealed by auditory brainstem and middle-latency evoked potentials. Eur J Neurosci 32:859–865.

Slabu L, Grimm S, Escera C (2012): Novelty detection in the human auditory brainstem. J Neurosci 32:1447–1452.

Sonnadara RR, Alain C, Trainor LJ (2006): Occasional changes in sound location enhance middle latency evoked responses. Brain Res 1076:187–192.

Sussman ES, Gumenyuk V (2005): Organization of sequential sounds in auditory memory. Neuroreport 16:1519–1523.

Sussman E, Winkler I (2001): Dynamic sensory updating in the auditory system. Cogn brain Res 12:431–439.

Sussman E, Ritter W, Vaughan HG, Vaughan HG Jr (1998): Predictability of stimulus deviance and the mismatch negativity. Neuroreport 9:4167–4170.

Taaseh N, Yaron A, Nelken I (2011): Stimulus-specific adaptation and deviance detection in the rat auditory cortex. PLoS One 6: e23369.

Takegata R, Huotilainen M, Rinne T, Näätänen R, Winkler I (2000): Changes in acoustic features and their conjunctions are processed by separate neuronal populations. Neuroreport 12: 525–529.

Tervaniemi M, Rytkönen M, Schröger E, Ilmoniemi RJ, Näätänen R (2001): Superior formation of cortical memory traces for melodic patterns in musicians. Learn Mem 8:295–300.

Uhrig L, Dehaene S, Jarraya B (2014): A hierarchy of responses to auditory regularities in the macaque brain. J Neurosci 34:1127–1132.

Ulanovsky N, Las L, Nelken I (2003): Processing of low-probability sounds by cortical neurons. Nat Neurosci 6:391–398.

Van Veen B, van Drongelen W, Yuchtman M, Suzuki A (1997): Localization of brain electrical activity via linearly constrained minimum variance spatial filtering. IEEE Trans Biomed Eng 44:867–880.

Wacongne C, Labyt E, van Wassenhove V, Bekinschtein T, Naccache L, Dehaene S (2011): Evidence for a hierarchy of predictions and prediction errors in human cortex. Proc Natl Acad Sci USA 108:20754–20759.

Warren JE, Wise RJS, Warren JD (2005): Sounds do-able: Auditory-motor transformations and the posterior temporal plane. Trends Neurosci 28:636–643.

Winkler I, Denham SL, Nelken I (2009): Modeling the auditory scene: Predictive regularity representations and perceptual objects. Trends Cogn Sci 13:532–540.

Yaron A, Hershenhoren I, Nelken I (2012): Sensitivity to complex statistical regularities in rat auditory cortex. Neuron 76:603–615.

Yvert B, Crouzeix A, Bertrand O, Seither-Preisler A, Pantev C (2001): Multiple supratemporal sources of magnetic and electric auditory evoked middle latency components in humans. Cereb cortex 11:411–423.

Zatorre R, Belin P, Penhune V (2002): Structure and function of auditory cortex: Music and speech. Trends Cogn Sci 6:37–46.